1 **MedPharmRes (MPR) TITLE PAGE**

2 **Upload this completed form to website with submission**

3

ARTICLE INFORMATION	Fill in information in each box below
Article Type	Research article
Article Title (within 20 words without abbreviations)	**Discovery of potent inhibitors of NS4B protein of dengue virus type 2 from natural compounds: An *in silico* approach**
Running Title (within 10 words)	Discovery of natural DENV-2 NS4B inhibitors
Author	Phat Nguyen Pham[1], Quynh Nguyen Nhu Le[1], Phuong Thuy Viet Nguyen[1]*
Affiliation	[1] Department of Pharmaceutical Information Technology, University of Medicine and Pharmacy at Ho Chi Minh City, Ho Chi Minh City, Vietnam
ORCID (for more information, please visit https://orcid.org)	
Competing interests	No potential conflict of interest relevant to this article was reported.
Funding sources State funding sources (grants, funding sources, equipment, and supplies). Include name and number of grant if available.	Not applicable.
Acknowledgements	The authors would like to thank Faculty of Pharmacy, University of Medicine and Pharmacy at Ho Chi Minh city, Viet Nam for their support.
Availability of data and material	Upon reasonable request, the datasets of this study can be available from the corresponding author.
Authors' contributions Please specify the authors' role using this form. Authors can't change and add items, but you can delete items that are not applicable.	Conceptualization: Phuong T V Nguyen Data curation: Phat N Pham, Quynh N N Le Formal analysis: Phat N Pham, Quynh N N Le Methodology: Phat N Pham Validation: Phuong T V Nguyen Investigation: Phat N Pham Writing - original draft: Quynh N N Le Writing - review & editing: Phuong T V Nguyen (All authors should be listed in this field.)

UNCORRECTED PROOF

Ethics approval and consent to participate	All procedures in this study were approved by the Institutional Review Board (IRB) of ABC University, Vietnam (ABC-IRB-2020-1205). OR Informed consent for publication of the images was obtained from the patient. OR Not applicable.

4

5 **CORRESPONDING AUTHOR CONTACT INFORMATION**

For the corresponding author (responsible for correspondence, proofreading, and reprints)	**Fill in information in each box below**
First name, middle initial, last name	Phuong Thuy Viet Nguyen
Email address – this is where your proofs will be sent	nvphuong@ump.edu.vn
Secondary Email address	
Address	Department of Pharmaceutical Information Technology, University of Medicine and Pharmacy at Ho Chi Minh City, Ho Chi Minh City, Vietnam
Cell phone number	+084-919520708
Office phone number	
Fax number	

6

7

UNCORRECTED PROOF

ABSTRACT

Introduction: Dengue fever is an annual infectious epidemic disease caused by the Dengue virus, mainly found in tropical and subtropical regions. Of which, Dengue virus type 2 (DENV2) has been a major cause of severe cases globally. Currently, NS4B is one of the promising targets of dengue drug discovery, as it is crucial for the virus life cycle and highly conserved among different dengue strains. However, up till now, no potent synthetic DENV2 NS4B inhibitors have entered clinical research due to toxicity profiles. Therefore, this study aimed to search for new DENV2 NS4B inhibitors from in-house phytochemical compound database based on integration of *in silico* approaches.

Methods: Initially, due to the lack of crystal structure of DENV2 NS4B protein, the 3D structure and binding site of this protein were predicted. Subsequently, virtual screening process was conducted through molecular docking and the most potential compounds in terms of binding affinity were selected for MDs and binding free energy calculation.

Results: The flavonoid compound D155, derived from *Valeriana hardwickii*, and the saponin compound D170, extracted from *Glinus oppositifolius*, exhibited good binding affinities and bound well in the binding site of DENV2 NS4B protein. Notably, MDs study revealed that these two compounds formed stable interactions with NS4B protein during 200 ns of simulation and had a binding free energy < -20 kcal/mol.

Conclusions: The findings suggested that D155 and D170 can be potential inhibitors targeting NS4B protein of DENV2. Further *in vitro* and *in vivo* studies are required to confirm their inhibitory activities.

Keywords: Dengue, Dengue type 2 or DENV2; NS4B protein; Natural compound; *in silico*

UNCORRECTED PROOF

1. INTRODUCTION

Dengue fever primarily occurs in tropical and subtropical regions and is caused by the Dengue virus (DENV) which belongs to the family Flaviviridae, genus *Flavivirus* [1]. According to the US statistics [2], dengue hemorrhagic fever is an annual epidemic with a mortality rate over 13% in untreated patient. Five serotypes of the dengue virus have been reported, namely DENV1, DENV2, DENV3, DENV4 and DENV5, with DENV2 being the main cause of major outbreaks and severe cases [3]. There is currently no specific antivirals has been approved for dengue therapeutic [4].

The genome of DENV2 comprises of a positive single-stranded RNA that is approximately 10,700 nucleotides long and can be directly translated into polyproteins [5]. These polyproteins are truncated into ten different proteins, which can be classified into two groups: structural proteins and non-structural proteins (NS). Structural proteins, including capsid protein, envelope protein, and membrane protein, are involved in virus entry and budding processes [5]. Non-structural proteins consist of seven proteins: NS1, NS2A, NS2B, NS3, NS4A, NS4B and NS5, which have been reported to contribute to the inhibition of signaling from interferon-α/β [5].

Among targets of dengue drug discovery, NS4B is the largest trans-membrane protein and shares high similarity among different DENV strains [4]. NS4B is particularly important due to its central role in the virus life cycle, such as: (i) inhibiting the interferon-α/β signaling; (ii) interacting with NS3 to regulate the function of the helicase enzyme; (iii) interacting with NS1 in virus replication; (iv) contributing to suppress the host's RNA interference response [4]. Several compounds, such as NITD-688, SDM25N, 14a, AM404 and spiropyrazolopyridone, have been studied *in vitro* and *in vivo* for their inhibitory effects on this protein [4]. However, none of these compounds have progressed to clinical research due to their high toxicity profiles.

Natural compounds have historically played a crucial role in drug development, particularly for cancer and infectious diseases [6]. These phytochemicals are characterized by their great structural diversity and complexity. Many investigation techniques have been utilized in drug discovery from natural source. In anti-dengue agents discovery, many medicinal plants, such as *Andrographis paniculata*, *Momordica charantia*, and *Schisandra chinensis*, have demonstrated promising anti-dengue effects through *in vitro* and *in vivo* studies [7]. Through *in silico* approaches, such as homology modelling, molecular docking and quantitative structure–activity relationship (QSAR), some phytochemical structures

UNCORRECTED PROOF

have been identified to be developed as novel NS4B inhibitors, including: eu-flavonoid, 1,3-benzodioxole, iso-flavonoid, and indole [8, 9].

Therefore, the objective of this study was to identify potential natural inhibitors of the NS4B protein of DENV2 using molecular docking and molecular dynamics simulations (MDs) approaches. The method initiated by modelling the NS4B protein structure and followed by screening in-house natural compounds using molecular docking. Molecular dynamics simulations and binding free energy calculation were combined to investigate the stability and flexibility of NS4B protein as well as protein-ligand complexes to select the most potential inhibitors for DENV2 NS4B.

2. MATERIALS AND METHODS

2.1. Generate the structure and predict the binding site of NS4B protein

2.1.1. Generate structure

Due to the lack of crystal structure of NS4B protein of DENV2, two methods were conducted to predict the structure of this protein:

(1) Template-based approach using homology modelling with SWISS-MODEL server (https://swissmodel.expasy.org) [10].

(2) Template-free approach using ColabFold 1.5.2 (https://colab.research) [11].

The UniProt database entry P29991, which represents the full polyprotein genome of DENV2, was used to obtain the sequence of the NS4B protein. Specifically, residues 2244 to 2491were extracted from P29991 (248 amino acids) to define the NS4B sequence (Figure 1). This sequence was then subjected to SWISS-MODEL server and ColabFold to generate 3D structure. In SWISS-MODEL, the structural template used for building model was selected in terms of a sequence identity of over 30% or a minimum sequence similarity of 0.4 between the NS4B protein and the template protein. In addition, ColabFold generated five high-quality structural models, and the first ranked model was chosen for further analysis.

Then, the protein structure was run MDs for 25 ns at temperature 300 K, pressure 1 bar to investigate the equilibrium structure using Gromacs 2022.5 [12]. The simulation results were analyzed based on the value of RMSD (root-mean-square-deviation). The equilibrium structure was obtained at the time that the RMSD value was below 2 Å (0.2 nm).

2.1.2. Binding site prediction

Using the obtained equilibrium structure of DENV2 NS4B, the binding site of this protein was determined by three methods, including CATSp v3.0 [13], P2Rank v2.4 [14], and blind docking with 73 compounds that have known to have activity against DENV2 or

UNCORRECTED PROOF

the NS4B protein of DENV2 from 30 articles [4, 15-43] (Structure and corresponding EC_{50} values (μM) listed in Supplementary Table 1).

Then, the final binding cavity was selected by comparing and overlapping the results from these three methods.

2.2. Molecular docking

Virtual screening process was performed through molecular docking on the structure of DENV2 NS4B and binding cavity obtained in the previous steps. The screening database included 286 in-house natural compounds which were collected from the Faculty of Pharmacy, University of Medicine and Pharmacy at Ho Chi Minh City, Vietnam (listed in Supplementary Table 2). The two-dimensional (2D) structures of ligands were drawn and converted to three-dimensional (3D) structures by ChemSketch [44] and Discovery Studio Visualizer version 2021 [45], respectively. After energy minimizing and converting to pdb format, these ligands were prepared for docking by using AutoDock Tools 1.5.6 package [46]. Later on, Autodock Vina software [47] was used for docking process with grid box parameters obtained from the prediction binding site process and were listed in **Table 1**. Molecular docking was also conducted for 16 reference compounds (listed in Supplementary Table 3). The docking results were analyzed based on two criteria, including binding affinity (kcal/mol) and interactions between ligand and residues in binding cavity. Compounds that had strong binding affinities (≤ -9.0 kcal/mol) and interactions with residues similar to interactions of the reference compounds were identified as promising compounds.

2.3. Molecular dynamics simulations

To further investigate the results of molecular docking, top five potential compounds were selected for MDs using Gromacs 2022.5 software [12]. The structures, including the complexes of NS4B protein-ligand and apo NS4B protein (free ligand), were run MDs during 50 ns using the all-atom CHARMM-36 force field. The process involved several stages, including topology preparation, generation of a dodecahedron simulation box, solvation of the system in water and adding ions to neutralize the system, energy minimization and system equilibration at a temperature of 300 K and a pressure of 1 bar within 1000 ps before running MDs. The simulation results were analyzed based on parameters such as the values of RMSD, RMSF (root-mean-square-fluctuation), Rg (radius of gyration), SASA (solvent-accessible surface area), and percentage of hydrogen bond occupancy. In particular, the hydrogen bond occupancy percentages were analyzed using the VMD software [48] to evaluate the interaction potential of ligands with the key residues. A hydrogen bond was defined by simple geometric criteria, which included a distance of less

UNCORRECTED PROOF

than 3.5 Å between the hydrogen donor (D) and acceptor (A) atoms, and an angle greater than 120° for D–H···A [49].

After the 50 ns MDs had been completed, the most stable NS4B protein-ligand complexes were further subjected to a longer simulation of 200 ns. The results were compared with the values of the apo NS4B protein under the same conditions and run time.

2.4. Binding free energy calculation

The binding energies of the complexes of the top hit compounds, obtained from the long-time scale MDs using the CHARMM-36 force field, were calculated by the gmx_MMPBSA package [50]. In this study, snapshots taken from the 200 ns MDs trajectory of each protein-ligand complex were used to calculate binding free energy through both MM/GBSA and MM/PBSA (Molecular Mechanics/ Generalized Born or Poisson-Boltzmann Surface Area) methods. The results from these approaches were compared and evaluated. The solute's dielectric constant was set to 1.0, with a temperature of 298 K and a salt concentration of 0.15 M. The free energies (ΔG_{bind}) for binding of the ligand to NS4B protein with ligand in solvent can be expressed as [51]:

$$\Delta G_{\text{bind}} = \Delta G_{\text{complex}} - (\Delta G_{\text{protein}} + \Delta G_{\text{ligand}}) \quad (1)$$

The equation (1) can be divided into the contributions of various interactions and represented as:

$$\Delta G_{\text{bind}} = \Delta H - T\Delta S = \Delta E_{\text{MM}} + \Delta G_{\text{solv}} - T\Delta S \quad (2)$$

in which:

$$\Delta E_{\text{MM}} = \Delta E_{\text{int}} + \Delta E_{\text{vdW}} + \Delta E_{\text{ele}} \quad (3)$$

$$\Delta G_{solv} = \Delta G_{\text{PB/GB}} + \Delta G_{\text{SA}} \quad (4)$$

$$\Delta G_{SA} = \gamma \cdot SASA + \Delta G_{\text{SA}} \quad (5)$$

In the above equations, ΔE_{MM}, ΔG_{solv} and $-T\Delta S$ refer to the changes in gas phase molecular mechanics energy, solvation free energy, and conformational entropy that occur during ligand binding, respectively. Due to the high computational cost, changes in conformational entropy ($-T\Delta S$) are typically neglected when calculating the relative binding free energies of similar ligands [51]. ΔE_{int} represents the internal bonded energy components, such as bond, angle, and dihedral energies, which are regarded as zero in a dynamic simulation [51]. E_{vdW} and ΔE_{ele} are the nonbonded *van der Waals* and the electrostatic interaction energy, respectively. ΔG_{solv} is the sum of the electrostatic solvation energy $\Delta G_{\text{PB/GB}}$ (polar component) and the nonpolar contribution ΔG_{SA} between the solute and the surrounding continuum solvent. The polar contribution is determined using the PB

UNCORRECTED PROOF

method with the level set function model [52] and the GB method with the GB-OBC2 model [53], while the nonpolar energy is typically estimated based on SASA.

3. RESULTS AND DISCUSSION

3.1. Generate the structure and predict the binding site of NS4B protein

3.1.1. Generate structure

With template-based approach, no 3D crystal protein structure retrieved from Protein Data Bank satisfied the criteria of identity > 30% or similarity > 0.4 (Supplementary Table 4) to be used as a template in the homology modeling method.

With template-free approach, a total of 150 sequences were obtained from performing multiple sequence alignment. The sequence with the highest identity and coverage (100%) was selected for NS4B protein structure generation. With this sequence, the protein model was generated by using ColabFold 1.5.2 (Figure 2). In order to ensure the stability and flexibility of the generated protein structure of DENV2 NS4B, MDs was run for this structure for 25 ns.

Analysis of the results revealed that the structure reached equilibrium at 16 ns (with the value of RMSD below 2 Å) and maintained stable oscillation until the end of the simulation (Figure 3). Therefore, the conformation of the NS4B protein of DENV2 at 16 ns was extracted and used for further steps.

3.1.2. Binding site prediction

Three approaches were used for prediction of binding site of DENV2 NS4B. First, using CASTp program (based on geometry), 35 binding cavities with their corresponding volumes were identified on the DENV2 NS4B protein. Among them, only cavity A1 was selected since it met the volume requirement over 300 $Å^3$. Secondly, with P2Rank program (based on machine learning), site B1 was chosen as it possessed the highest score of 55.02 and a probability of 0.983. Finally, blind docking identified two binding sites on the NS4B protein: C1 and C2. Among them, cavity C1 was selected because there were 69 out of 73 ligands bound to. Table 2 provided a summary of the important parameters of A1, B1, and C1.

In combination, the results from the three approaches of predicting binding cavity, the selected binding site consisted of 30 amino acids (Figure 4). Among them, 29 amino acids (including: Trp38, Tyr41, Ala42, Thr45, Thr46, Thr49, Pro50, Lys86, Asp88, Gly90, Val91, Leu94, Pro162, Glu165, Lys166, Gly169, Gln170, Thr203, Pro209, Gly210, Asn214, Thr215, Thr216, Phe237, Ser238, Lys241, Asn242, Arg247, Arg248) were found in all three

UNCORRECTED PROOF

methods while 1 amino acid, His117, was retained due to its deep position within the cavity and its involvement in numerous interactions during the blind docking method. Two key residues were predicted to be Glu165 and Lys166 based on analysis of interactions between protein and 16 reference compounds with their EC_{50} values ranging from about 10^{-6} to 8.1 μM in blind docking [4, 15, 16, 38, 40, 41] (Supplementary Table 3).

3.2. Molecular docking

Molecular docking was conducted for a total of 286 natural compounds into the DENV2 NS4B protein, resulting in the discovery of 33 compounds with the strong binding affinities (≤ -9.0 kcal/mol) from different structural groups: alkaloids (1 substance), flavonoids (15 substances), and terpenoids (17 substances). The alkaloid compound D240 (-9.2 kcal/mol) exhibited strong binding affinity within the binding cavity and created many hydrogen bonds and hydrophobic interactions. However, D240 did not form the same interactions as any reference compounds, and it also did not interact with the key residues Glu165 or Lys166 (Figure 5). Therefore, D240 was not selected for the next step.

In flavonoid group, all the compounds with good binding affinities were glycosides, including 3 structural groups: eu-flavonoids (9 substances), iso-flavonoids (5 substances) and neo-flavonoids (1 substance). Although these phytochemicals were capable of forming numerous hydrogen bonds and hydrophobic interactions with residues in binding sites, only D113, D155, and D203 had interactions with key residues or similar to interactions observed with the reference compounds. D113 (-9.2 kcal/mol) was classified as an iso-flavone compound belonging to the iso-flavonoid group with a phenyl branch at position C3 and a glycol group at position C7. This compound formed a hydrogen bond between the hydroxyl group (-OH) on the glycol part and hydrogen in Glu165. It also had many hydrophobic interactions with amino acids, including Lys166 (Figure 6).

Compound D155 (-9.4 kcal/mol) belonged to the eu-flavonoid group and was classified as a flavone compound. It had a phenyl branch at C2 and two glycol substituents at position C7 of chroman skeleton. This compound interacted with the binding cavity through hydrogen bond with Glu165 and π-Alkyl bond between the chroman ring and Lys166 (Figure 7).

Compound D203 (-9.4 kcal/mol) was an iso-flavone compound. D203 created multiple hydrogen bonds with amino acids (Gln170, Gly210, Asn214, Asn242) at the hydroxyl groups (-OH) on the phenyl ring and the glycol part. These interactions were similar to those observed for the reference compound F35 (NITD-688), which was a pan-serotype inhibitor and exhibited anti-DENV2 activity with an EC_{50} of 0.008 μM [4].

UNCORRECTED PROOF

Additionally, hydrophobic interactions were also analyzed between D203 and three amino acids Trp38, Ala42, and Lys166 (Figure 8).

Terpenoids with good binding affinities belonged to 3 groups: sesterterpenes (3 substances), triterpenes (12 substances) and saponins (2 substances). Among them, D170 and D239 (2 saponins) were the two substances chosen as the most promising. Compound D170 (-10.3 kcal/mol) was a saponin that consisted of a short glycol part connected to a sulfate group. This arrangement led to the formation of a hydrogen bond between the ether group (-O-) and hydrogen in the hydroxyl group (-OH) on Thr216. The aglycon part of D170 included an amyrin skeleton with multiple methoxy substituents, resulting in hydrophobic interactions with the amino acid Trp38. Notably, these interactions closely resembled those observed with the F42 reference compound (AM404), which was an active metabolite of paracetamol and exhibited anti-DENV2 activity with an EC_{50} of 3.6 µM [4]. Additionally, D170 also interacted with Lys86 and Lys166 through hydrogen bonds (Figure 9).

Compound D239 (-9.0 kcal/mol) with saponin structure demonstrated significant interactions with amino acids in the binding site. The glycol part of D239 formed multiple hydrogen bonds, particularly with key residue Glu165. Additionally, the aglycon part of D239 contained an aromatic ring that was deeply inserted into the cavity, resulting in a hydrophobic interaction with key residue Lys166, as depicted in Figure 10.

Additionally, the sesterterpene and triterpene compounds, typically D126 with binding affinity of -11 kcal/mol, exhibited strong binding affinities but were unable to form interactions with the residues within the binding cavity (as shown in Figure 11). As a result, they were excluded from the final screening results.

3.3. Molecular dynamics simulations

The results of the simulation process of 5 complexes between protein-ligand (D113, D155, D170, D203, D239) and apo-protein were presented in Figure 12. By examining the RMSD, RMSF, Rg, and SASA values of these complexes compared to apo-protein and the stability of each ligand through their heavy atoms, our study highlighted the ability to form stable complexes of two compounds D155 and D170 during 50 ns of simulation. These two protein-ligand complexes exhibited both protein and ligand RMSD deviations of less than 0.2 nm after 25 ns and the oscillation remained stable until the end of the simulation. Additionally, the RMSF values of the residues within the binding cavity were lower than the values observed for the apo-protein. Moreover, both Rg and SASA values were more stable

UNCORRECTED PROOF

compared to the apo protein. Therefore, the two complexes of the NS4B protein with the ligands D155 and D170 were selected for further hydrogen bond occupancy analysis (Table 3) and long-time scale MDs (Figure 13).

A rapid assessment of the drug-like and ADMET properties of these 5 ligands was carried out by using the ADMETlab 3.0 web server [54] and the predicted results were presented in the Supplementary Table 5. The results showed that all compounds satisfied at least one drug-likeness rule, with no PAINS (Pan Assay Interference Compounds) alerts and no serious toxicity. However, D170 performed good absorption compared to other compounds.

3.4. Binding free energy calculation

The binding free energy analysis for the NS4B protein and its complexes with the top hit ligands, D155 and D170, were derived from 200 ns MDs trajectories (from frame 1 to 20001 with interval of 10). The ΔG_{bind} values and energy components were presented in Table 4. Their fluctuations over time were depicted in Figure 13. In the first 25 ns of the simulations, the binding free energies tended to decrease because the complexes progressed toward equilibrium. After reaching equilibrium, the free energy remained negative until the end of 200 ns of simulation. These results indicated that the interactions between the two ligands and the NS4B protein were formed and stayed stable throughout the simulation.

4. DISCUSSION

Phytochemicals have long been used in traditional medicine to treat various diseases and have been shown to inhibit viral replication and transcription [55]. Various plant-derived products have been extensively studied against viruses such as herpes, human immunodeficiency virus (HIV), influenza, hepatitis, and SARS-CoV-2 [55]. However, there is still limited exploration of phytochemicals for the inhibition of viruses like dengue virus [55]. Therefore, in this study, structure-based virtual screening through molecular docking and molecular dynamics simulations was conducted to evaluate 286 natural compounds targeting the NS4B protein of DENV2 to identify potential anti-dengue agents.

Despite the lack of crystal structure of NS4B protein of DENV2, its topology has been investigated so far. In previous NMR study, an 11-helix model was proposed for the secondary structure of the DENV NS4B protein with 6 of these helices remaining membrane-buried [56]. The N-terminal region comprised a small helix (α1) and disordered

UNCORRECTED PROOF

residues [56]. The C-terminal region contained four small helices (α8, α8', α9, α9'), where α8 and α8' were not fully membrane-buried, α9 and α9' could interchange for mobility [56]. Similar to these, the ColabFold model predicted a total of 11 helices, out of which one small helix in the N-terminal and four helices in the C-terminal region (Figure 2). In previous studies on the unstructured biology of proteins of dengue virus, the NS4B protein of DENV2 exhibited a disorder propensity of 14.5% [57]. These included disordered N- and C-terminal tails and the cytosolic loop region [57], which were considered as intrinsically disordered protein regions (IDPRs) of NS4B protein of DENV2. Long MDs exceeding 1 μs for the C-terminal in an aqueous environment revealed similar findings [58]. IDPRs exist as dynamic conformational ensembles with varying levels of residual structure over simulation time, which affected the RMSD fluctuations, ranging from collapsed (molten globule-like) to partially collapsed (pre-molten globule-like), and even highly extended (coil-like) conformations [57]. These regions were predicted to be unsuitable for stable drug binding. Therefore, to reduce complexity and computational resources, the structure at the single frame of NS4B protein, after both the non-IDPRs and IDPRs of the protein had reached a stable state, was extracted for further analyses. In this study, the predicted NS4B protein was run molecular dynamics simulations (MDs) to obtain the stable conformation and more accurate structure of NS4B. This structure reached equilibrium stage from 16 ns of MD, thus the NS4B conformation at the 16 ns frame was the stable conformation. Clustering analysis also showed that the conformation at the 16 ns also belonged to the first representative structure cluster of NS4B. Thus, this structure of NS4B at 16 ns was used for virtual screenings in the next stage.

The most stable MD conformation and the best binding pocket are two different aspects. The most stable MD conformation does not necessarily correspond to the best binding pocket. Therefore, utilizing the stable conformation of the NS4B protein structure, the best binding pocket was identified by using a combination of three methods based on distinct principles: (1) CATSp, which identified pockets based on the 3D structure of the protein and spatial geometry, (2) traditional machine learning that utilized the random forest algorithm implemented in P2Rank, and (3) blind docking of known bioactive compounds across the entire target protein. The optimal binding pocket was selected by integrating the results from these three approaches.

73 compounds possessing the activity against DENV2 or the NS4B protein of DENV2 from 30 articles [4, 15-43] (Structure and corresponding EC_{50} values (μM) listed in Supplementary Table 1 were selected for docking. Among the reference compounds, the

UNCORRECTED PROOF

compound F11 corresponds to JNJ-A07 (as shown in Supplementary Table 1). It is a pan-serotype dengue virus inhibitor targeting the NS3–NS4B interaction [1]. In the original study conducted by Kaptein et al. in 2021 [1], JNJ-A07 was evaluated for its antiviral activity against DENV2 in six cell lines and various genotypes of all four DENV serotypes. This compound exhibited antiviral activity at nano- to picomolar concentrations across various cell lines and against the diversity of known genotypes and serotypes of the dengue virus, including DENV2. Although the EC_{50} value of F11 for DENV2 was not precisely determined, the activity of JNJ-A07 was also confirmed in a mice model of DENV2 infection [1]. For this reason, F11 was used as a reference compound for this study.

Through the criteria including ligand binding affinities, binding modes and binding interactions between the NS4B protein and 33 compounds, the top five promising compounds were identified as D113 (-9.2 kcal/mol), D155 (-9.4 kcal/mol), D170 (-10.3 kcal/mol), D203 (-9.4 kcal/mol), and D239 (-9.0 kcal/mol) (Figure 14). These compounds shared two key characteristics, including the presence of glycol group with multiple hydroxyl (-OH) substituents and a bulky aglycon group that increased the overall hydrophobicity of the molecules. The glycol substituents enabled the formation of hydrogen bonds between the compounds and the surrounding hydrophilic residues within the binding cavity of the NS4B protein. Additionally, the hydrophobic aglycon group allowed the compounds to attach deeply and interact with the residues in the binding pocket, especially the key residue Lys166, which likely contributed to their strong binding affinities.

The molecular docking analysis showed that compound D155 created stable interactions including hydrogen bonds with His117 and Glu165, as well as hydrophobic interaction with Lys166. After simulation, these hydrogen bond interactions remained consistently stable with high occupancy, reaching 188.15% for the interaction with His117 and 267.41% for the interaction with Glu165. However, the hydrophobic interaction with Lys166 was replaced by hydrogen bond at a frequency of 148.42%. Furthermore, after MDs, this compound also formed new additional hydrogen bonds with other amino acids, such as Lys24, Trp38, Thr45, Lys86 and Thr216, with a frequency greater than 70%. On the other hand, D170 demonstrated hydrogen bonds with Lys86, Lys166 and Thr216 during molecular docking. However, after the MDs, only the hydrogen bond with Thr216 was maintained and new hydrogen bond was formed with Glu165 with occupancy of 198.98% and 225.09%, respectively. In particular, binding free energy calculation revealed that both complexes had negative binding free energies, regardless of the two calculation approaches, indicating their ability to form stable complexes with the NS4B protein until the end of the simulations.

UNCORRECTED PROOF

Combining the results from docking, MDs, and ΔG_{bind} values, D155 and D170 were selected as the most potential NS4B inhibitors.

Currently, there has been no investigation on the potential of compounds D155 and D170 to inhibit the NS4B protein or DENV strains. However, in previous studies, these compounds have shown multiple promising activities. D155 (Neodiosmin) is a type of flavonoid that can be derived from the butanol extract of the *Valeriana hardwickii* plant, which belongs to the Valerian family (Valerianaceae) or citrus plants (*Citrus bergamia, Citrus aurantium, Cirus australasica*…). It has shown promise to be an anti-SARS-CoV-2 agent (*in silico and in vitro*) [59] and antioxidant (*in vitro*) [60]. D170 (Spergulin A) is a saponin extracted from the ethanol extract of *Glinus oppositifolius* Molluginaceae. It has shown the ability to resist the parasite *Leishmania donovani* (*in vitro*) [61] and antibacterial (*E. coli, H. influenzae, S. aureus, etc.)* (*in vitro*) [62].

In addition to the promising findings regarding the inhibitory potential of two natural compounds against the NS4B protein of DENV2, the study has some limitations that should be noted. In this research, the structural analysis of the NS4B protein of DENV2 was obtained by predicted and then used for MDs to obtain more accurate and equilibrium and stable conformational structure, However, MDs were investigated in an aqueous environment, which does not account for the influence of the lipid bilayer in maintaining the equilibrium of the protein, particularly in IDPRs. Thus, the natural compound database used for screening in this study included only an in-house collection of over 200 natural compounds. Expanding this library to include a broader range of natural compounds could enhance the scope of future investigations targeting the NS4B protein of DENV2. Finally, the inhibitory potential of the compounds was predicted only for the monomeric state of the NS4B protein, without considering the effects of interactions between NS4B and other proteins, including NS3, NS4A, NS5, NS1, and the dimeric state of NS4B.

5. CONCLUSIONS

In this study, molecular docking and molecular dynamics simulations approaches were applied to discover potential inhibitors of NS4B protein of DENV2. Due to the lack of crystal structure, template-based and template-free approach were applied to predict the tertiary structure of DENV2 NS4B protein. The obtained 3D structure of NS4B reached equilibrium after 16 ns of MDs. Based on three binding site prediction methods, a ligand binding cavity of NS4B consisting of 30 amino acids was identified. Virtual screening of natural compounds by molecular docking and analyzing stability by MDs and ΔG_{bind} values showed that two compounds D155 (Neodiosmin) and D170 (Spergulin A) had potential in

UNCORRECTED PROOF

inhibiting NS4B protein of DENV2. Overall, this study suggests that Neodiosmin and Spergulin A can be further investigated to be used as potential therapeutic treatment on DENV2 NS4B protein.

6. ACKNOWLEDGEMENTS

We would like to thank the University of Medicine and Pharmacy at Ho Chi Minh City, Vietnam for supporting for this research.

Author contribution

Phat Nguyen Pham: generate structure, predict binding site, virtual screening.

Quynh Nguyen Nhu Le: molecular dynamics simulations, binding free energy calculations.

Phuong Thuy Viet Nguyen: study design, manuscript editing.

Funding

This research received no external funding.

Conflict of interest (If any)

The authors declare that they have no conflict of interest.

Ethics approval

None to declare

Supplementary Materials

Supplementary materials are only available online from:
https://doi.org/10.32895/UMP.MPR.9.3.x

UNCORRECTED PROOF

REFERENCES

1. Guzman MG, Halstead SB, Artsob H, Buchy P, Farrar J, Gubler DJ, et al. Dengue: a continuing global threat. Nature Reviews Microbiology. 2010;8(12):S7-S16. doi: 10.1038/nrmicro2460.
2. Clinical Considerations for Dengue Virus Infection [Internet]. 2022 [cited 06 July 2023]. Available from: https://emergency.cdc.gov/newsletters/coca/083022.htm
3. Halstead SB. Dengue. The Lancet. 2007;370(9599):1644-52. doi: 10.1016/S0140-6736(07)61687-0.
4. Li Q, Kang C. Dengue virus NS4B protein as a target for developing antivirals. Front Cell Infect Microbiol. 2022;12:959727. Epub 20220809. doi: 10.3389/fcimb.2022.959727. PubMed PMID: 36017362; PubMed Central PMCID: PMCPMC9398000.
5. Perera R, Kuhn RJ. Structural proteomics of dengue virus. Current Opinion in Microbiology. 2008;11(4):369-77. doi: https://doi.org/10.1016/j.mib.2008.06.004.
6. Atanasov AG, Waltenberger B, Pferschy-Wenzig E-M, Linder T, Wawrosch C, Uhrin P, et al. Discovery and resupply of pharmacologically active plant-derived natural products: A review. Biotechnology Advances. 2015;33(8):1582-614. doi: https://doi.org/10.1016/j.biotechadv.2015.08.001.
7. Altamish M, Khan M, Baig MS, Pathak B, Rani V, Akhtar J, et al. Therapeutic Potential of Medicinal Plants against Dengue Infection: A Mechanistic Viewpoint. ACS Omega. 2022;7(28):24048-65. doi: 10.1021/acsomega.2c00625.
8. Adawara SN, Shallangwa GA, Mamza PA, Abdulkadir I. In-silico modeling of inhibitory activity and toxicity of some indole derivatives towards designing highly potent dengue virus serotype 2 NS4B inhibitors. Journal of Chemistry Letters. 2022;3(1):46-56. doi: 10.22034/jchemlett.2022.336894.1065.
9. Qaddir I, Rasool N, Hussain W, Mahmood S. Computer-aided analysis of phytochemicals as potential dengue virus inhibitors based on molecular docking, ADMET and DFT studies. Journal of Vector Borne Diseases. 2017;54(3).
10. Waterhouse A, Bertoni M, Bienert S, Studer G, Tauriello G, Gumienny R, et al. SWISS-MODEL: homology modelling of protein structures and complexes. Nucleic Acids Research. 2018;46(W1):W296-W303. doi: 10.1093/nar/gky427.
11. Mirdita M, Schütze K, Moriwaki Y, Heo L, Ovchinnikov S, Steinegger M. ColabFold: making protein folding accessible to all. Nature Methods. 2022;19(6):679-82. doi: 10.1038/s41592-022-01488-1.
12. Bauer P, Hess, B., Lindahl, E. GROMACS 2022.5 (Version 2022.5). 2023.

UNCORRECTED PROOF

13. Tian W, Chen C, Lei X, Zhao J, Liang J. CASTp 3.0: computed atlas of surface topography of proteins. Nucleic Acids Research. 2018;46(W1):W363-W7. doi: 10.1093/nar/gky473.
14. Krivák R, Hoksza D. P2Rank: machine learning based tool for rapid and accurate prediction of ligand binding sites from protein structure. Journal of Cheminformatics. 2018;10(1):39. doi: 10.1186/s13321-018-0285-8.
15. Balasubramanian A, Pilankatta R, Teramoto T, Sajith AM, Nwulia E, Kulkarni A, et al. Inhibition of dengue virus by curcuminoids. Antiviral Research. 2019;162:71-8. doi: https://doi.org/10.1016/j.antiviral.2018.12.002.
16. Baltina LA, Tasi Y-T, Huang S-H, Lai H-C, Baltina LA, Petrova SF, et al. Glycyrrhizic acid derivatives as Dengue virus inhibitors. Bioorganic & Medicinal Chemistry Letters. 2019;29(20):126645. doi: https://doi.org/10.1016/j.bmcl.2019.126645.
17. Bodenreider C, Beer D, Keller TH, Sonntag S, Wen D, Yap L, et al. A fluorescence quenching assay to discriminate between specific and nonspecific inhibitors of dengue virus protease. Analytical Biochemistry. 2009;395(2):195-204. doi: https://doi.org/10.1016/j.ab.2009.08.013.
18. Brecher M, Li Z, Liu B, Zhang J, Koetzner CA, Alifarag A, et al. A conformational switch high-throughput screening assay and allosteric inhibition of the flavivirus NS2B-NS3 protease. PLOS Pathogens. 2017;13(5):e1006411. doi: 10.1371/journal.ppat.1006411.
19. Byrd Chelsea M, Dai D, Grosenbach Douglas W, Berhanu A, Jones Kevin F, Cardwell Kara B, et al. A Novel Inhibitor of Dengue Virus Replication That Targets the Capsid Protein. Antimicrobial Agents and Chemotherapy. 2013;57(1):15-25. doi: 10.1128/aac.01429-12.
20. de Sousa LRF, Wu H, Nebo L, Fernandes JB, da Silva MFdGF, Kiefer W, et al. Flavonoids as noncompetitive inhibitors of Dengue virus NS2B-NS3 protease: Inhibition kinetics and docking studies. Bioorganic & Medicinal Chemistry. 2015;23(3):466-70. doi: https://doi.org/10.1016/j.bmc.2014.12.015.
21. Estoppey D, Lee CM, Janoschke M, Lee BH, Wan KF, Dong H, et al. The Natural Product Cavinafungin Selectively Interferes with Zika and Dengue Virus Replication by Inhibition of the Host Signal Peptidase. Cell Reports. 2017;19(3):451-60. doi: 10.1016/j.celrep.2017.03.071.
22. Kaptein Suzanne JF, De Burghgraeve T, Froeyen M, Pastorino B, Alen Marijke MF, Mondotte Juan A, et al. A Derivate of the Antibiotic Doxorubicin Is a Selective Inhibitor

UNCORRECTED PROOF

of Dengue and Yellow Fever Virus Replication In Vitro. Antimicrobial Agents and Chemotherapy. 2010;54(12):5269-80. doi: 10.1128/aac.00686-10.

23. Kiat TS, Pippen R, Yusof R, Ibrahim H, Khalid N, Rahman NA. Inhibitory activity of cyclohexenyl chalcone derivatives and flavonoids of fingerroot, Boesenbergia rotunda (L.), towards dengue-2 virus NS3 protease. Bioorganic & Medicinal Chemistry Letters. 2006;16(12):3337-40. doi: https://doi.org/10.1016/j.bmcl.2005.12.075.
24. Kounde CS, Yeo H-Q, Wang Q-Y, Wan KF, Dong H, Karuna R, et al. Discovery of 2-oxopiperazine dengue inhibitors by scaffold morphing of a phenotypic high-throughput screening hit. Bioorganic & Medicinal Chemistry Letters. 2017;27(6):1385-9. doi: https://doi.org/10.1016/j.bmcl.2017.02.005.
25. Liu H, Wu R, Sun Y, Ye Y, Chen J, Luo X, et al. Identification of novel thiadiazoloacrylamide analogues as inhibitors of dengue-2 virus NS2B/NS3 protease. Bioorganic & Medicinal Chemistry. 2014;22(22):6344-52. doi: https://doi.org/10.1016/j.bmc.2014.09.057.
26. Lu D, Liu J, Zhang Y, Liu F, Zeng L, Peng R, et al. Discovery and optimization of phthalazinone derivatives as a new class of potent dengue virus inhibitors. European Journal of Medicinal Chemistry. 2018;145:328-37. doi: https://doi.org/10.1016/j.ejmech.2018.01.008.
27. Niyomrattanakit P, Chen Y-L, Dong H, Yin Z, Qing M, Glickman JF, et al. Inhibition of Dengue Virus Polymerase by Blocking of the RNA Tunnel. Journal of Virology. 2010;84(11):5678-86. doi: 10.1128/jvi.02451-09.
28. Osman H, Idris NH, Kamarulzaman EE, Wahab HA, Hassan MZ. 3,5-Bis(arylidene)-4-piperidones as potential dengue protease inhibitors. Acta Pharmaceutica Sinica B. 2017;7(4):479-84. doi: https://doi.org/10.1016/j.apsb.2017.04.009.
29. Patkar Chinmay G, Larsen M, Owston M, Smith Janet L, Kuhn Richard J. Identification of Inhibitors of Yellow Fever Virus Replication Using a Replicon-Based High-Throughput Assay. Antimicrobial Agents and Chemotherapy. 2009;53(10):4103-14. doi: 10.1128/aac.00074-09.
30. Poh MK, Yip A, Zhang S, Priestle JP, Ma NL, Smit JM, et al. A small molecule fusion inhibitor of dengue virus. Antiviral Research. 2009;84(3):260-6. doi: https://doi.org/10.1016/j.antiviral.2009.09.011.
31. Raut R, Beesetti H, Tyagi P, Khanna I, Jain SK, Jeankumar VU, et al. A small molecule inhibitor of dengue virus type 2 protease inhibits the replication of all four dengue virus

UNCORRECTED PROOF

serotypes in cell culture. Virology Journal. 2015;12(1):16. doi: 10.1186/s12985-015-0248-x.

32. Saleem HN, Batool F, Mansoor HJ, Shahzad-ul-Hussan S, Saeed M. Inhibition of Dengue Virus Protease by Eugeniin, Isobiflorin, and Biflorin Isolated from the Flower Buds of Syzygium aromaticum (Cloves). ACS Omega. 2019;4(1):1525-33. doi: 10.1021/acsomega.8b02861.
33. Salin NH, Hariono M, Khalili NSD, Zakaria, II, Saqallah FG, Mohamad Taib MNA, et al. Computational study of nitro-benzylidene phenazine as dengue virus-2 NS2B-NS3 protease inhibitor. Front Mol Biosci. 2022;9:875424. Epub 20221117. doi: 10.3389/fmolb.2022.875424. PubMed PMID: 36465554; PubMed Central PMCID: PMCPMC9715268.
34. Shimizu H, Saito A, Mikuni J, Nakayama EE, Koyama H, Honma T, et al. Discovery of a small molecule inhibitor targeting dengue virus NS5 RNA-dependent RNA polymerase. PLOS Neglected Tropical Diseases. 2019;13(11):e0007894. doi: 10.1371/journal.pntd.0007894.
35. Timiri AK, Selvarasu S, Kesherwani M, Vijayan V, Sinha BN, Devadasan V, et al. Synthesis and molecular modelling studies of novel sulphonamide derivatives as dengue virus 2 protease inhibitors. Bioorganic Chemistry. 2015;62:74-82. doi: https://doi.org/10.1016/j.bioorg.2015.07.005.
36. Tomlinson SM, Malmstrom RD, Russo A, Mueller N, Pang Y-P, Watowich SJ. Structure-based discovery of dengue virus protease inhibitors. Antiviral Research. 2009;82(3):110-4. doi: https://doi.org/10.1016/j.antiviral.2009.02.190.
37. van Cleef KWR, Overheul GJ, Thomassen MC, Kaptein SJF, Davidson AD, Jacobs M, et al. Identification of a new dengue virus inhibitor that targets the viral NS4B protein and restricts genomic RNA replication. Antiviral Research. 2013;99(2):165-71. doi: https://doi.org/10.1016/j.antiviral.2013.05.011.
38. Whitby K, Pierson Theodore C, Geiss B, Lane K, Engle M, Zhou Y, et al. Castanospermine, a Potent Inhibitor of Dengue Virus Infection In Vitro and In Vivo. Journal of Virology. 2005;79(14):8698-706. doi: 10.1128/jvi.79.14.8698-8706.2005.
39. Wu H, Bock S, Snitko M, Berger T, Weidner T, Holloway S, et al. Novel Dengue Virus NS2B/NS3 Protease Inhibitors. Antimicrobial Agents and Chemotherapy. 2015;59(2):1100-9. doi: 10.1128/aac.03543-14.

UNCORRECTED PROOF

40. Xie X, Wang Q-Y, Xu Hao Y, Qing M, Kramer L, Yuan Z, et al. Inhibition of Dengue Virus by Targeting Viral NS4B Protein. Journal of Virology. 2011;85(21):11183-95. doi: 10.1128/jvi.05468-11.
41. Yang J-M, Chen Y-F, Tu Y-Y, Yen K-R, Yang Y-L. Combinatorial Computational Approaches to Identify Tetracycline Derivatives as Flavivirus Inhibitors. PLOS ONE. 2007;2(5):e428. doi: 10.1371/journal.pone.0000428.
42. Ye N, Chen H, Wold EA, Shi P-Y, Zhou J. Therapeutic Potential of Spirooxindoles as Antiviral Agents. ACS Infectious Diseases. 2016;2(6):382-92. doi: 10.1021/acsinfecdis.6b00041.
43. Yin Z, Chen Y-L, Schul W, Wang Q-Y, Gu F, Duraiswamy J, et al. An adenosine nucleoside inhibitor of dengue virus. Proceedings of the National Academy of Sciences. 2009;106(48):20435-9. doi: doi:10.1073/pnas.0907010106.
44. Advanced Chemistry Development IAL. ChemSketch (Version 2022). 2022.
45. BIOVIA DS. Discovery Studio Visualiser (Version 2021) 2021.
46. Morris GM, Huey R, Lindstrom W, Sanner MF, Belew RK, Goodsell DS, et al. AutoDock4 and AutoDockTools4: Automated docking with selective receptor flexibility. J Comput Chem. 2009;30(16):2785-91. doi: 10.1002/jcc.21256. PubMed PMID: 19399780; PubMed Central PMCID: PMCPMC2760638.
47. Trott O, Olson AJ. AutoDock Vina: improving the speed and accuracy of docking with a new scoring function, efficient optimization, and multithreading. J Comput Chem. 2010;31(2):455-61. doi: 10.1002/jcc.21334. PubMed PMID: 19499576; PubMed Central PMCID: PMCPMC3041641.
48. Humphrey W, Dalke A, Schulten K. VMD: visual molecular dynamics. J Mol Graph. 1996;14(1):33-8, 27-8. doi: 10.1016/0263-7855(96)00018-5. PubMed PMID: 8744570.
49. Rungrotmongkol T, Nunthaboot N, Malaisree M, Kaiyawet N, Yotmanee P, Meeprasert A, et al. Molecular insight into the specific binding of ADP-ribose to the nsP3 macro domains of chikungunya and Venezuelan equine encephalitis viruses: molecular dynamics simulations and free energy calculations. J Mol Graph Model. 2010;29(3):347-53. Epub 20101029. doi: 10.1016/j.jmgm.2010.09.010. PubMed PMID: 21036084.
50. Valdes-Tresanco MS, Valdes-Tresanco ME, Valiente PA, Moreno E. gmx_MMPBSA: A New Tool to Perform End-State Free Energy Calculations with GROMACS. J Chem Theory Comput. 2021;17(10):6281-91. Epub 20210929. doi: 10.1021/acs.jctc.1c00645. PubMed PMID: 34586825.

UNCORRECTED PROOF

588 51. Wang E, Sun H, Wang J, Wang Z, Liu H, Zhang JZH, et al. End-Point Binding Free
589 Energy Calculation with MM/PBSA and MM/GBSA: Strategies and Applications in
590 Drug Design. Chem Rev. 2019;119(16):9478-508. Epub 20190624. doi:
591 10.1021/acs.chemrev.9b00055. PubMed PMID: 31244000.
592 52. Wang J, Cai Q, Xiang Y, Luo R. Reducing grid-dependence in finite-difference Poisson-
593 Boltzmann calculations. J Chem Theory Comput. 2012;8(8):2741-51. Epub 20120618.
594 doi: 10.1021/ct300341d. PubMed PMID: 23185142; PubMed Central PMCID:
595 PMCPMC3505068.
596 53. Onufriev A, Bashford D, Case DA. Exploring protein native states and large-scale
597 conformational changes with a modified generalized born model. Proteins.
598 2004;55(2):383-94. doi: 10.1002/prot.20033. PubMed PMID: 15048829.
599 54. Fu L, Shi S, Yi J, Wang N, He Y, Wu Z, et al. ADMETlab 3.0: an updated
600 comprehensive online ADMET prediction platform enhanced with broader coverage,
601 improved performance, API functionality and decision support. Nucleic Acids Res.
602 2024;52(W1):W422-W31. doi: 10.1093/nar/gkae236. PubMed PMID: 38572755;
603 PubMed Central PMCID: PMCPMC11223840.
604 55. Ghildiyal R, Prakash V, Chaudhary VK, Gupta V, Gabrani R. Phytochemicals as
605 Antiviral Agents: Recent Updates. Plant-derived Bioactives. 2020:279 - 95.
606 56. Li Y, Wong YL, Lee MY, Li Q, Wang QY, Lescar J, et al. Secondary Structure and
607 Membrane Topology of the Full-Length Dengue Virus NS4B in Micelles. Angew Chem
608 Int Ed Engl. 2016;55(39):12068-72. Epub 20160824. doi: 10.1002/anie.201606609.
609 PubMed PMID: 27554985.
610 57. Meng F, Badierah RA, Almehdar HA, Redwan EM, Kurgan L, Uversky VN.
611 Unstructural biology of the Dengue virus proteins. FEBS J. 2015;282(17):3368-94.
612 Epub 20150715. doi: 10.1111/febs.13349. PubMed PMID: 26096987.
613 58. Bhardwaj T, Kumar P, Giri R. Investigating the conformational dynamics of Zika virus
614 NS4B protein. Virology. 2022;575:20-35. Epub 20220821. doi:
615 10.1016/j.virol.2022.08.005. PubMed PMID: 36037701.
616 59. Babaeekhou L, Ghane M, Abbas-Mohammadi M. In silico targeting SARS-CoV-2 spike
617 protein and main protease by biochemical compounds. Biologia. 2021;76(11):3547-65.
618 doi: 10.1007/s11756-021-00881-z.
619 60. Cioni E, Migone C, Ascrizzi R, Muscatello B, De Leo M, Piras AM, et al. Comparing
620 Metabolomic and Essential Oil Fingerprints of Citrus australasica F. Muell (Finger Lime)

UNCORRECTED PROOF

621 Varieties and Their In Vitro Antioxidant Activity. Antioxidants. 2022;11(10). doi:
622 10.3390/antiox11102047.
623 61. Banerjee S, Mukherjee N, Gajbhiye RL, Mishra S, Jaisankar P, Datta S, et al.
624 Intracellular anti-leishmanial effect of Spergulin-A, a triterpenoid saponin of Glinus
625 oppositifolius. Infect Drug Resist. 2019;12:2933-42. Epub 20190917. doi:
626 10.2147/idr.S211721. PubMed PMID: 31571946; PubMed Central PMCID:
627 PMCPMC6756365.
628 62. Assimon VA, Shao H, Garneau-Tsodikova S, Gestwicki JE. Concise synthesis of
629 spergualin -inspired molecules with broad-spectrum antibiotic activity.
630 MedChemComm. 2015;6(5):912-8. doi: 10.1039/C4MD00572D.

631

UNCORRECTED PROOF

Table 1. Parameters of grid box for molecular docking of DENV2 NS4B

Parameter	Center_x	Center_y	Center_z	Size_x	Size_y	Size_z	Spacing
Value (Å)	100.577	83.641	45.819	28	28	28	1.00

Table 2. The results of binding cavities from CASTp, P2Rank and blind docking

Cavity	**Features**
A1 (41 residues)	**Area (Å^2):** 612.926 **Volume (Å^3):** 539.760 Trp38, Thr39, Tyr41, Ala42, Val43, Thr45, Thr46, Thr49, Pro50, Ser85, Lys86, Met87, Asp88, Ile89, Gly90, Val91, Leu94, His117, Pro162, Lys163, Glu165, Lys166, Gln167, Gly169, Gln170, Thr203, Pro209, Gly210, Arg211, Asn214, Thr215, Thr216, Gly234, Phe237, Ser238, Lys241, Asn242, Asn245, Thr246, Arg247, Arg248
B1 (30 residues)	**Score:** 55.02 **Probability:** 0.983 Trp38, Thr39, Tyr41, Ala42, Thr45, Thr46, Thr49, Pro50, Lys86, Asp88, Gly90, Val91, Leu94, Pro162, Glu165, Lys166, Gly169, Gln170, Thr203, Pro209, Gly210, Asn214, Thr215, Thr216, Phe237, Ser238, Lys241, Asp242, Arg247, Arg248
C1 (43 residues)	Trp38, Tyr41, Ala42, Thr45, Thr46, Thr49, Pro50, Arg53, His54, Glu57, Asn58, Gly81, Trp82, Pro83, Leu84, Ser85, Lys86, Met87, Asp88, Ile89, Gly90, Val91, Leu94, His117, Pro162, Lys163, Glu165, Lys166, Gln167, Gly169, Gln170, Thr203, Pro209, Gly210, Asn214, Thr215, Thr216, Phe237, Ser238, Lys241, Asn242, Arg247, Arg248

UNCORRECTED PROOF

638 **Table 3.** The percentage of hydrogen bond occupancy between ligands (D155, D170) and
639 amino acids in the binding cavity of NS4B protein during 50 ns MDs

Compounds	Donor	Acceptor	Percentage (%)
D155	Lig155-Side	Glu165-Side	267.41
	Lig155-Side	Asp88-Side	229.09
	Lig155-Side	Thr45-Side	155.30
	Lys166-Side	Lig155-Side	148.42
	Lig155-Side	Thr216-Side	123.83
	His117-Side	Lig155-Side	105.86
	Trp38-Side	Lig155-Side	102.64
	Lig155-Side	Tyr41-Side	97.02
	Gln170-Side	Lig155-Side	85.61
	Lig155-Side	His117-Side	82.29
	Lig155-Side	Trp38-Side	81.99
	Thr216-Side	Lig155-Side	77.27
D170	Lys241-Side	Lig170-Side	293.26
	Lig170-Side	Glu165-Side	225.09
	Thr216-Side	Lig170-Side	198.98
	Lig170-Side	Asp88-Side	139.12
	Thr216-Main	Lig170-Side	99.46
	Lig170-Side	Thr45-Side	95.48
	Lys86-Main	Lig170-Main	71.81
	Lig170-Side	Lys86-Main	70.63
	Lig170-Side	Leu84-Main	70.37

640
641
642 **Table 4.** The calculation of binding free energy results of 2 top hit compounds

Complex	NS4B-D155		NS4B-D170	
	MM/GBSA	MM/PBSA	MM/GBSA	MM/PBSA
ΔE_{vdW} (kcal/mol)	-47.08 ± 5.47	-47.08 ± 5.47	-57.4 ± 4.72	-57.4 ± 4.72
ΔE_{elec} (kcal/mol)	-54.34 ± 18.60	-54.34 ± 18.6	-65.98 ± 15.39	-65.98 ± 15.39
$\Delta G_{PB/GB}$ (kcal/mol)	64.56 ± 12.42	83.62 ± 14.98	71.82 ± 8.75	87.88 ± 10.32
ΔG_{SASA} (kcal/mol)	-7.18 ± 0.61	-5.54 ± 0.32	-8.52 ± 0.53	-6.00 ± 0.17
ΔG_{gas} (kcal/mol)	-101.42 ± 17.92	-101.42 ± 17.92	-123.38 ± 15.65	-123.38 ± 15.65
ΔG_{solv} (kcal/mol)	57.38 ± 12.29	78.08 ± 14.87	63.30 ± 8.49	81.88 ± 10.28
ΔG_{bind} (kcal/mol)	-44.04 ± 8.00	-23.34 ± 6.56	-60.08 ± 8.70	-41.50 ± 7.92

643
644

UNCORRECTED PROOF

>sp|P29991|POLG_DEN27 Genome polyprotein OS=Dengue virus type 2 (strain 16681-PDK53) OX=31635 PE=1 SV=1
NEMGFLEKTKKDLGLGSIATQQPESNILDIDLRPASAWTLYAVATTFVTPMLRHSIENSSVNVSLTAIANQATVLMGL
GKGWPLSKMDIGVPLLAIGCYSQVNPTTLTAALFLLVAHYAIIGPALQAKASREAQKRAAAGIMKNPTVDGITVIDLD
PIPYDPKFEKQLGQVMLLVLCVTQVLMMRTTWALCEALTLATGPISTLSEGNPGRFWNTTIAVSMANIFRGSYLAG

Figure 1. Amino acids sequence of NS4B protein of DENV2

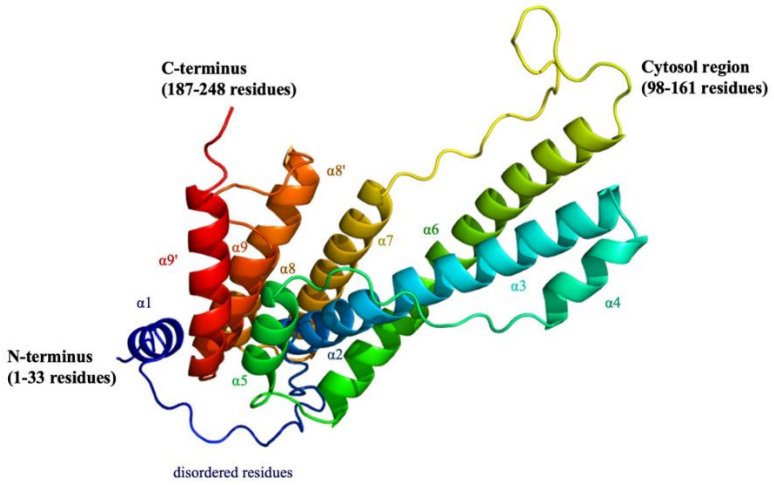

Figure 2. The predicted 3D structure of DENV2 NS4B protein

UNCORRECTED PROOF

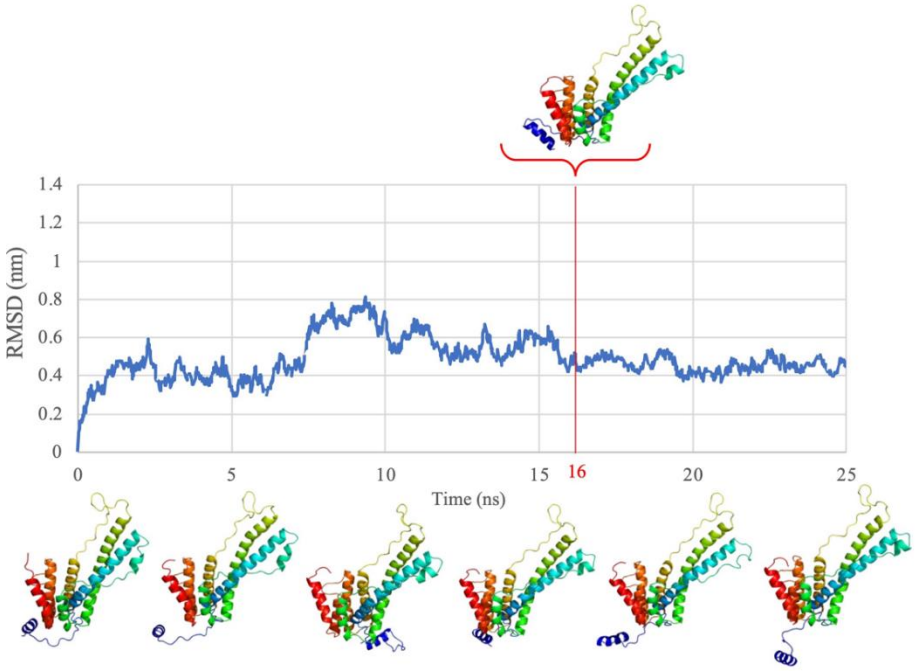

652

653 **Figure 3.** RMSDs value and conformations at each time of NS4B protein of DENV2

654 during 25 ns MDs

655

656

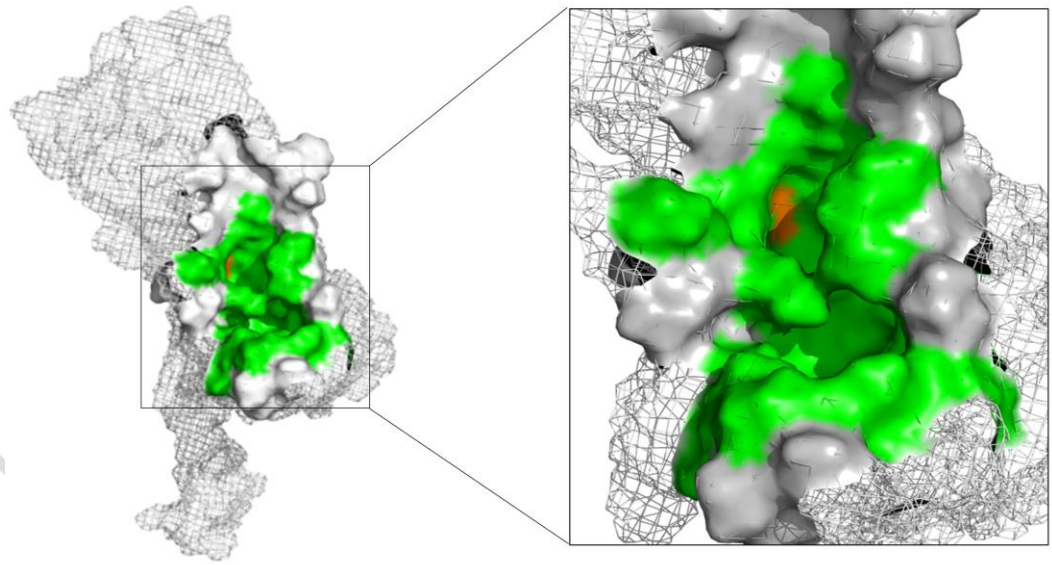

657

658 **Figure 4.** Binding site of NS4B protein of DENV2 (green: common residues between 3

659 approaches, orange: amino acid His117, gray: different predicted results)

660

661

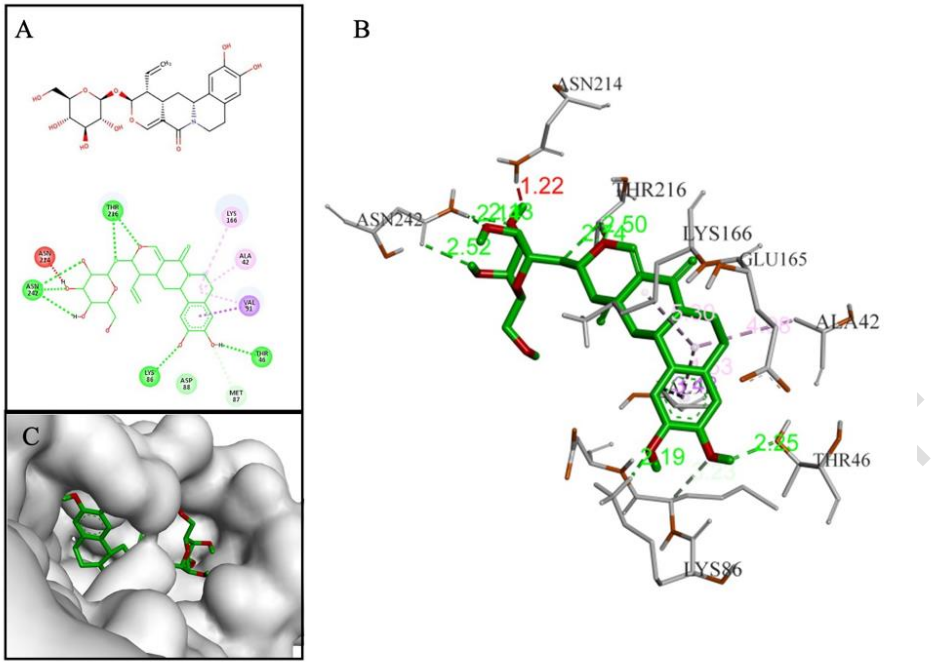

Figure 5. Interactions between D240 and amino acids in the binding cavity: (A) 2D, (B) 3D, (C) Binding mode of D240 in cavity

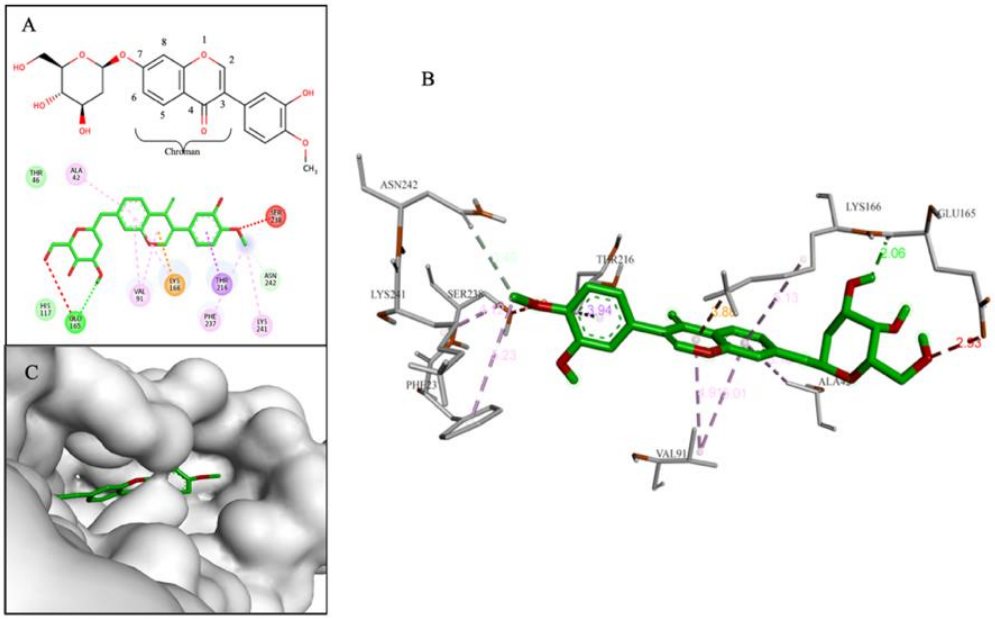

Figure 6. Interactions between D113 and amino acids in the binding cavity: (A) 2D, (B) 3D, (C) Binding mode of D113 in cavity

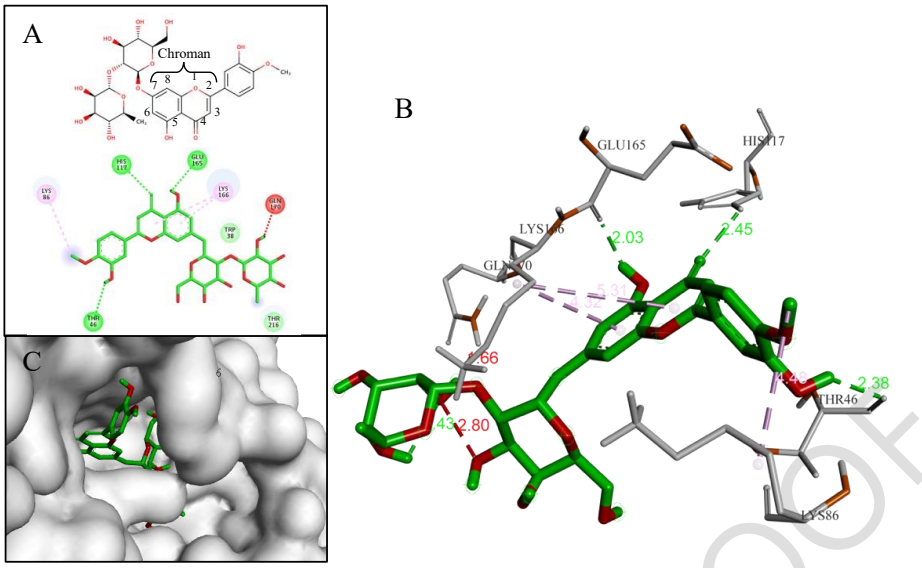

Figure 7. Interactions between D155 and amino acids in the binding cavity: (A) 2D, (B) 3D, (C) Binding mode of D155 in cavity

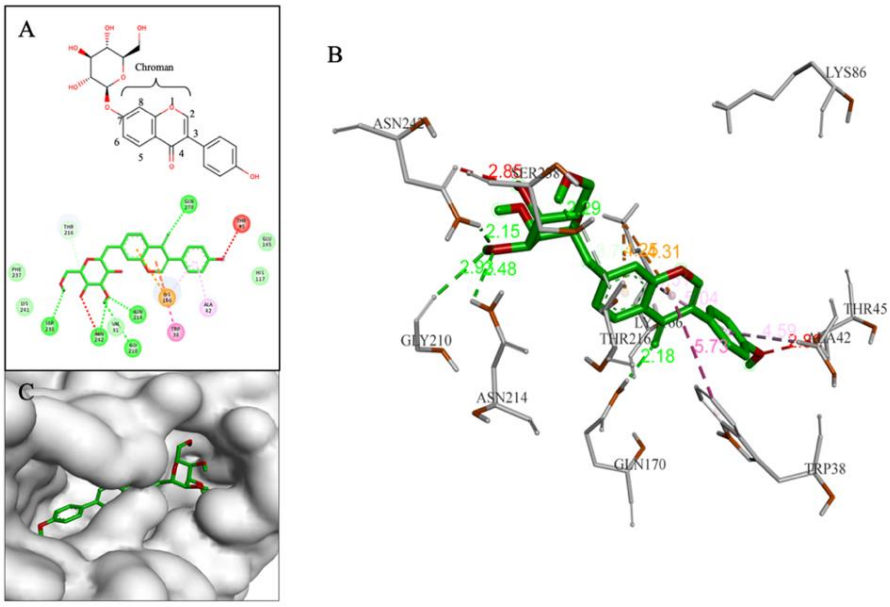

Figure 8. Interactions between D203 and amino acids in the binding cavity: (A) 2D, (B) 3D, (C) Binding mode of D203 in cavity

PROOF

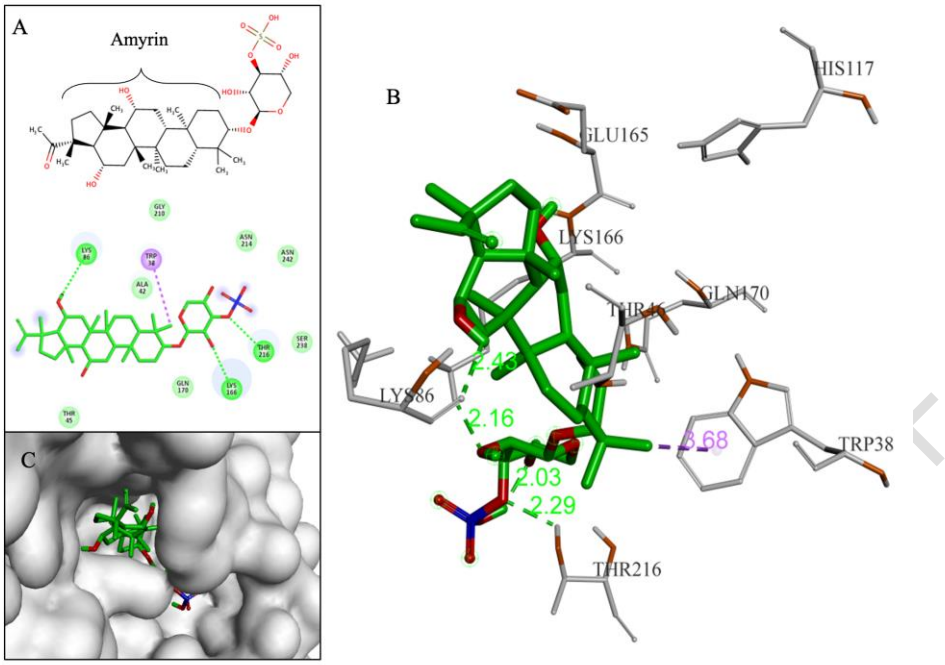

679

680 **Figure 9.** Interactions between D170 and amino acids in the binding cavity: (A)

681 2D, (B) 3D, (C) Binding mode of D170 in cavity

682

683

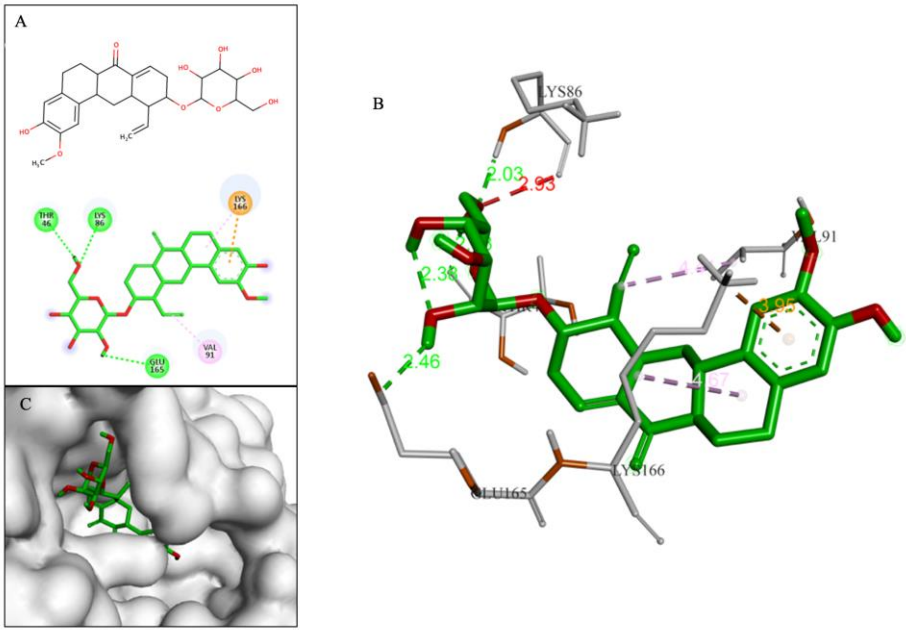

684

685 **Figure 10.** Interactions between D239 and amino acids in the binding cavity: (A)

686 2D, (B) 3D, (C) Binding mode of D239 in cavity

687

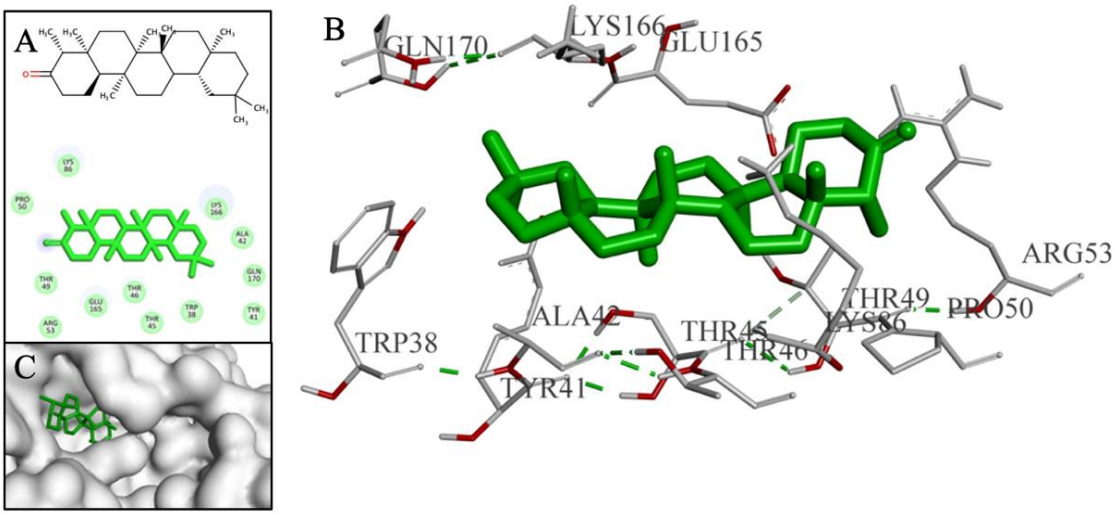

688

689 **Figure 11.** Interactions between D126 and amino acids in the binding cavity: (A) 2D, (B)

690 3D, (C) Binding mode of D126 in cavity

691

UNCORRECTED PROOF

693 **Figure 12.** Results of molecular dynamics simulations of DENV2 NS4B apo-protein
694 compared to 5 protein-ligand complexes (A: Protein backbone RMSD, B: Ligand RMSD,
695 C: RMSF, D: Rg, E: SASA) during 50 ns MDs
696

UNCORRECTED

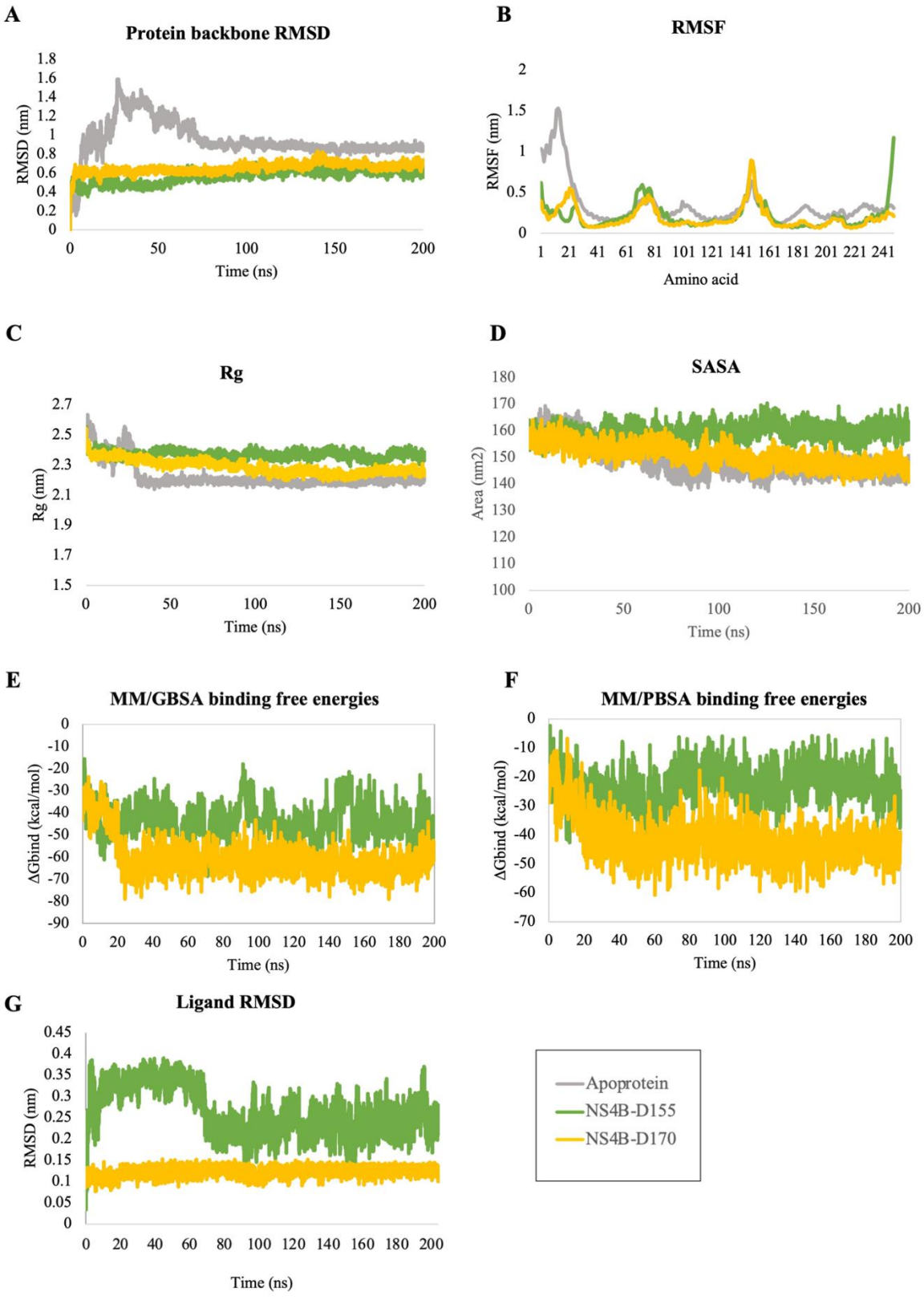

Figure 13. Results of molecular dynamics simulations of apo-protein compared to complexes of D155 and D170 (A: Protein backbone RMSD, B: RMSF, C: Rg, D: SASA, G: Ligand RMSD) and the binding free energy variation (E: MM/GBSA, F: MM/PBSA) during 200 ns

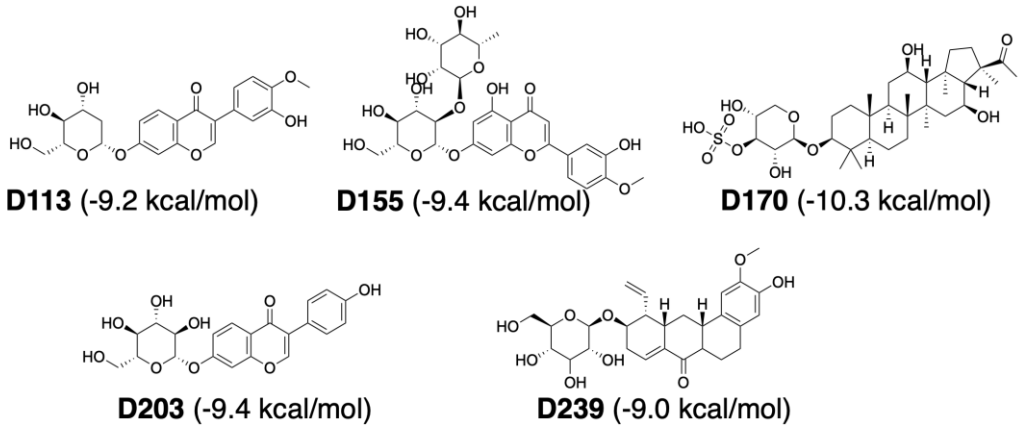

Figure 14. The structures and binding affinities of five promising compounds against DENV2 NS4B protein

UNCORRECTED PROOF